International High Performance Buildings Conference

School of Mechanical Engineering

2010

Estimating a Building Airflow Network using CO2 Measurements from a Distributed Sensor Network

Y. Lisa Chen
Drexel University

Jin Wen
Drexel University

Chen, Y. Lisa and Wen, Jin, "Estimating a Building Airflow Network using CO2 Measurements from a Distributed Sensor Network" (2010). *International High Performance Buildings Conference.* Paper 37.
http://docs.lib.purdue.edu/ihpbc/37

Estimating a Building Airflow Network using CO_2 Measurements from a Distributed Sensor Network

Y. Lisa CHEN[1]*, Jin WEN[2]

[1]Department of Civil, Architectural, and Environmental Engineering, Drexel University
Philadelphia, PA, USA
215-895-2280 (tel), yhc22@drexel.edu

[1]Department of Civil, Architectural, and Environmental Engineering, Drexel University
Philadelphia, PA, USA
215-895-4911 (tel), jinwen@drexel.edu

* Corresponding Author

ABSTRACT

An appropriate estimate of a building airflow network, which consists of infiltration and interzonal airflow, is important when determining indoor air quality, energy use, and for detecting contaminants. The objective of this study was to estimate the airflow network of a commercial building using CO_2 as a tracer. CO_2 is naturally present in the environment and is generated inside buildings by occupants. In Part I of this study, various sets of "perfect" CO_2 measurements were simulated under different occupancy schedules. In Part II of this study, the effect of CO_2 sensor uncertainty on airflow estimation was evaluated. Linear least squares was used in both parts of this study to estimate the building airflow network. This study demonstrated (1) the feasibility of using CO_2 as a tracer to estimate a building airflow network and (2) that a good estimate of the building airflow network can be made even under sensor uncertainty.

1. INTRODUCTION

An appropriate estimate of a building airflow network, which consists of infiltration and interzonal airflow, is important when determining indoor air quality, energy use, and for detecting contaminants. Fan pressurization tests are used to determine the airtightness of a building envelope, which is characteristic of the envelope construction. Tracer gas tests, on the other hand, are used to determine the infiltration through a building envelope under specific outdoor and indoor conditions. Tracer gas tests can also be used to determine interzonal airflows.

ASTM Standard E779 specifies test conditions for blower-door tests and is intended for single-zone buildings or multi-zone buildings that can be considered a single-zone (ASTM, 2003). Canadian Standard CGSB149.15 specifies testing conditions for a fan pressurization test using a building's own air handling system (CGSB, 1999). It has been applied to commercial buildings with limitations (Jeong *et al.*, 2008). Bahnfleth *et al.* (1999) compared these two test standards in two multi-zone, multi-story buildings. The researchers found that neither method was easy to implement. Wind and stack effects were difficult to control in multi-story buildings. Further, the sealing of leakage paths between floors via shaft penetrations was challenging. Therefore, the results of the fan pressurization tests may be inaccurate.

ASTM Standard E741 specifies test conditions for tracer gas tests, as well as how to then determine air exchange rates (ASTM, 2000). Studies in the literature using CO_2 as a tracer have only been performed on single-zone or small multi-zone residences (Aglan, 2003; Lu *et al.*, 2010; Penman, 1980; Penman *et al.*, 1982; Roulet *et al.*, 2002;

Smith, 1988; Yan *et al.*, 2007). Most of these tests determined overall air exchange rates with the outdoors and not the specific airflow rate through the building envelope or between zones (interzonal airflow). In order to estimate interzonal airflow rates, either multiple tracers are needed (Miller *et al.*, 1997) or multiple tracer tests must be performed (Afonso *et al.*, 1986).

1.1 Study Objectives

The objective of this study was to estimate the airflow network of a commercial building using CO_2 as a tracer. It offers several advantages over the traditional blower-door and tracer gas tests just discussed. First, this study presents a method that can be implemented on multi-zone, commercial buildings, which is currently challenging given their size and the complexity of their building airflow network. Second, the method presented is able to determine airflow rates across the building envelope in each zone and also between zones. Third, the use of CO_2 is advantageous as it is a naturally present tracer. CO_2 sensors are readily available and relatively inexpensive compared to the equipment needed to measure a traditional tracer gas such as SF_6. And lastly, the method presented provides a fast estimate of the building airflow network. It requires less time to set-up than a traditional blower-door or tracer gas test and has the potential to determine a building airflow network in real-time.

1.2 Study Applications

This building airflow network estimation method presented in this study has several applications. First, it can be used to determine the building airtightness at specific parts of a building, not just the overall building airtightness. Second, once the building airflow network is estimated, it can be used to provide a quick estimate of the dispersion of other unmeasured contaminants. Third, an understanding of the building airflow network can provide insight into the pressure distribution of a building. This information is critical in spaces such as laboratories and hospitals. Lastly, it can be used for building commissioning.

2. STUDY METHODS

In Part I of this study, various sets of "perfect" CO_2 measurements were simulated under different occupancy schedules. In Part II of this study, the effect of CO_2 sensor uncertainty on airflow estimation was evaluated. Linear least squares was used in both parts of this study to estimate the building airflow network.

2.1 Synthetic Test Building

In lieu of experimental data, a three-zone commercial building was modeled in CONTAM (Walton *et al.*, 2005). Figure 1 shows the location of Zones A (common area), B (office), and C (conference room), along with their respective volumes. The exterior wall is modeled as brick veneer with a leakage property of 1.14 cm^2/m^2. The interior walls are modeled with leakage of 1.12 cm^2/m^2. The inoperable closed windows are modeled with leakage 0.86 cm^2/m of sash. The interior open doors are modeled as 2.1 m^2 openings. One-way flow through each of these leakage paths is governed by a power-law equation of the form $F = K(\Delta P)^n$, where F is the airflow rate (kg/s), ΔP is the pressure difference calculated by CONTAM (Pa), and K and n are empirical constants. In this study, K=1 and n=0.65 for all of the leakage paths. The leakage properties of each leakage path, along with air density, are then used to convert F (kg/s) to Q (m^3/s).

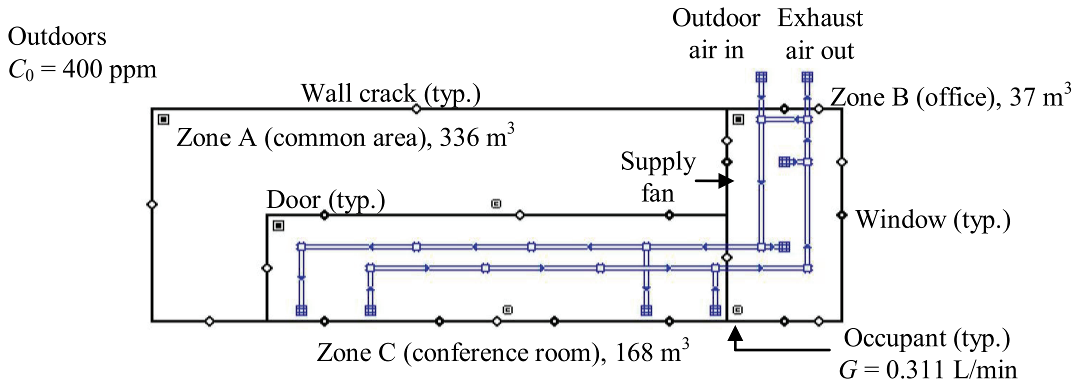

Figure 1: CONTAM model of three-zone test building.

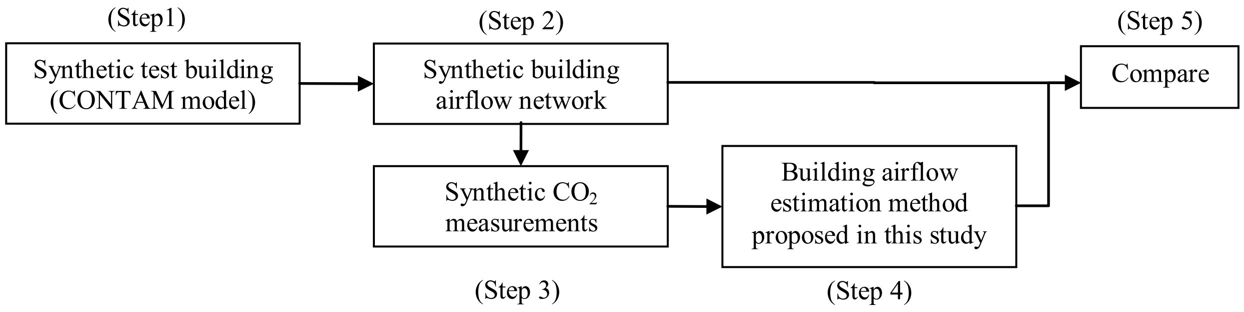

Figure 2: Flow diagram of study process.

A recirculation ventilation system was modeled with 20% outdoor air. The location of the outdoor air intake and total exhaust are shown in Figure 1. The supply fan delivers 4 m^3/h (145 cfm) to Zone B and 20 m^3/h (690 cfm) to Zone C, which are approximately 7 air changes per hour (ACH). Because Zone A was not mechanically ventilated and has a relatively large volume, the whole building air exchange rate is about 1 ACH. The figure shows the location of ductwork, diffusers, and exhausts. CO_2 is present in the outdoors (Zone 0) with a constant concentration of 400 ppm (DOC, 2010). CO_2 is generated by occupants in each zone at a rate of $G = 0.311$ L/min (ASHRAE, 1990).

Figure 2 summarizes the study process. In lieu of experimental data, the first step was to generate synthetic CO_2 measurements using CONTAM (Step 1). CONTAM first determines the pressure distribution. It then utilizes nonlinear pressure relationships, such as power-law equations, to determine the airflow rate through each leakage path and ductwork (Step 2). This synthetic building airflow network is then used to calculate synthetic CO_2 measurements (Step 3). This study then utilized linear least squares to back-estimate the building airflow network in Step 4 using the synthetic CO_2 measurements provided by CONTAM in Step 3. Lastly, the estimated building airflow network from Step 4 is compared to the one that actually generated the synthetic CO_2 measurements (CONTAM model, Step 2). Keep in mind that CONTAM utilizes nonlinear relationships between pressure and airflow to calculate airflow, whereas in this study, linear relationships between contaminant concentration and airflows were utilized to back-calculate airflow.

2.2 Building Airflow Network

The building airflow network can be estimated using the general contaminant mass balance equation is given in Equation (1). For this study, synthetic steady-state CO_2 measurements are available from CONTAM. Therefore, the left hand side of Equation (1) is zero. The use of transient measurements is saved for future work.

$$V_i \frac{dC_i}{dt} = 0 = \sum_{j \neq i} Q_{ji} C_j - \sum_{j \neq i} Q_{ij} C_i + \sum G_i \qquad (1)$$

Q_{ji} is the airflow rate from zone j to zone i (m^3/s), Q_{ij} is the airflow rate from zone i to zone j (m^3/s), C_j is the CO_2 concentration in zone j (kg/m^3), C_i is the CO_2 concentration in zone i (kg/m^3), and ΣG_i is the total CO_2 generated in zone i (kg/s). Thus, for N zones, the system of contaminant mass balance equations can be written as:

$$-\mathbf{G} = \mathbf{QC} \qquad (2)$$

where **Q** are the parameters to be estimated (building airflow network), **C** are the CO_2 concentrations in each of the N zones, the supply concentration, C_S, and the ambient concentration, C_0. **B** are sources of CO_2 in each of the N zones. Equation (2) can be expanded as:

$$-\begin{bmatrix} \sum G_1 \\ \sum G_2 \\ \cdots \\ \sum G_N \end{bmatrix} = \begin{bmatrix} -\sum_j Q_{1-j} & Q_{2-1} & \cdots & Q_{N-1} \\ Q_{1-2} & -\sum_j Q_{2-j} & & Q_{N-2} \\ \cdots & \cdots & \cdots & \cdots \\ Q_{1-N} & Q_{2-N} & \cdots & -\sum_j Q_{N-j} \end{bmatrix} \begin{bmatrix} C_1 \\ C_2 \\ \cdots \\ C_N \\ C_S \\ C_0 \end{bmatrix} \quad (3)$$

In order to estimate the parameters, **Q**, the system of equations should be just- or over-determined. Thus, various occupancy schedules were modeled to generate different sets of CO_2 data. Airflow remained constant. The occupancy schedules modeled are given in Table 1. Thus, as an example, ΣG_A (total CO_2 generated in Zone A) would be 1·0.311 L/min, ΣG_B (total CO_2 generated in Zone B) would be 1·0.311 L/min, and ΣG_C (total CO_2 generated in Zone C) would be 5·0.311 L/min for Test 1. The resulting steady-state CO_2 concentrations are given in Table 2. In Tests 1-6, Zone A had the highest steady-state CO_2 concentration, even though it had the same occupancy as Zone B, because it was not mechanically ventilated. The more total occupants inside the synthetic building, the higher the steady-state CO_2 concentrations were (see Tests 1 and 9).

Table 1: Number of occupants modeled in CONTAM.

	Test 1	Test 2	Test 3	Test 4	Test 5	Test 6	Test 7	Test 8	Test 9
Zone A	1	1	1	1	1	1	1	1	1
Zone B	1	1	1	1	1	1	2	3	4
Zone C	5	4	3	2	1	0	1	2	3
Total	7	6	5	4	3	2	4	6	8

Table 2: Synthetic steady-state CO_2 measurements (ppm) calculated by CONTAM.

	Test 1	Test 2	Test 3	Test 4	Test 5	Test 6	Test 7	Test 8	Test 9
Zone A	786	741	695	650	604	558	627	696	765
Zone B	720	687	653	620	588	554	669	784	900
Zone C	698	653	607	562	516	471	539	608	677
Supply	611	583	555	527	499	471	522	573	625

2.3 Parameter Estimation

The parameters, **Q**, were estimated using linear least squares, which minimizes a function, *J*:

$$J = \left| \mathbf{Q}\mathbf{C} + \mathbf{G} \right|^2 \quad (4)$$

which is the absolute difference between the left and right hand side of Equation (2). **Q** must: (a) satisfy air mass balance in each zone (incoming air – outgoing air = 0); (b) be non-negative; and (c) satisfy additional known conditions. The additional known conditions were: (c-1) supply airflow rates into Zones B and C were provided, as was the incoming outdoor air and total exhausted airflow rates; and (c-2) since Zone A was not mechanically ventilated, its supply and exhaust airflow rates were zero.

Part I of this study consisted of using "perfect" CO_2 measurements taken directly from the CONTAM model. Thus, Equation (4) was used in parameter estimation. Part II of this study consisted of observing the effects of CO_2 sensor uncertainty on airflow estimation. Therefore, **C** in Equation (4) was replaced with $\tilde{\mathbf{C}}$, where $\tilde{\mathbf{C}} = \mathbf{C} \pm \varepsilon$. ε is the sensor uncertainty, which was assumed to be 5% of the "perfect" measurement. A Monte Carlo simulation with 1,000 iterations was employed to observe the effect of CO_2 sensor uncertainty on airflow estimation. For each

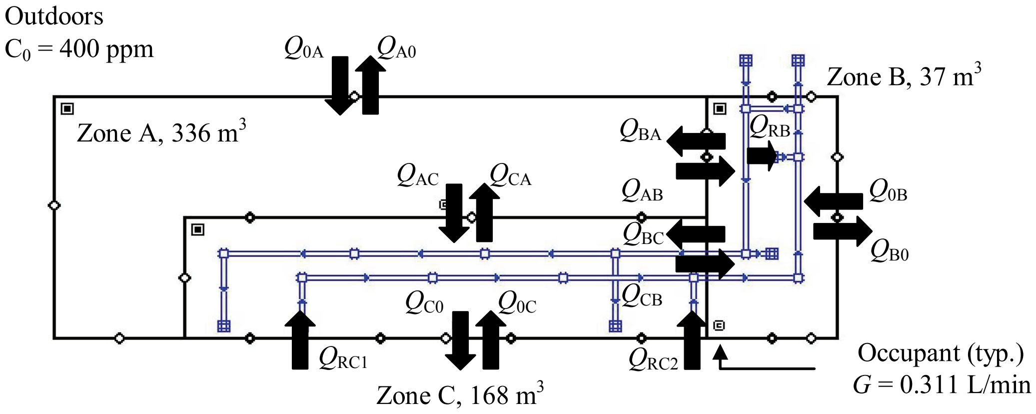

Figure 3: Building model showing parameters (airflow rates) estimated.

iteration, a single error value is sampled to determine $\tilde{\mathbf{C}}$. Thus, at the end of 1,000 iterations, the building airflow network will include mean (μ) and standard deviation values (σ) (reported as min and max values, which are μ-σ and μ+σ, respectively). The results of Part I and II are presented in the following section.

3. RESULTS

Figure 3 shows that 14 unknown parameters (airflow rates) were determined. There are two exhausts in Zone C (Q_{RC1} and Q_{RC2}), but only the total exhaust rate, Q_{RC}, was estimated. The airflow rate between two zones, including the outdoors, was the total airflow rate through all of the leakage paths between them. For example, there were two open doors and two interior wall leakage paths between Zones A and C. However, the airflow rate that was estimated between them was represented only by Q_{AC} or Q_{CA}. Each of the leakage paths in CONTAM was modeled as one-way flow, and each parameter must be non-negative (an imposed constraint). Therefore, only one of each pair of airflows between two zones will have a non-negative value. For example, between Zones A and C, either Q_{AC} or Q_{CA} will be non-negative and the other zero. In real buildings, two-way flow in leakage paths may exist between two zones. This situation is saved for future work.

3.1 Part I: Parameter Estimation using Perfect Sensor Measurements

Table 3 shows that airflow estimates from parameter estimation are mostly in good agreement with the synthetic values from CONTAM. The airflow estimates met all of the required constraints. Specifically, they (a) satisfied air mass balance in each zone (last six rows of Table 3), (b) were all non-negative, and (c) only one of each pair of airflows between two zones had a non-negative value.

The mean absolute difference in estimated airflows was 0.50 m^3/h (17 cfm), which is < 1 ACH difference in any zone. The largest percentage difference in estimated airflows was for Q_{C0} (100%), Q_{B0} (81%), and Q_{RB} (48%). Though these differences were considerable, steady-state CO_2 concentrations calculated using the estimated airflows differed <1% with those calculated by the CONTAM model. Thus, even relatively large differences in the estimation of the building airflow network resulted in small, if not negligible, differences in the calculation (or prediction) of contaminant concentration. Therefore, it could be concluded that CO_2 can be used as a tracer to estimate a building airflow network when steady-state measurements are available. A similar estimation procedure using transient CO_2 measurements is saved for future work.

3.2 Part II: Parameter Estimation using Sensor Measurements with Uncertainty

Table 4 shows the airflow estimates from parameter estimation using sensor measurements with uncertainty. Instead of a single value for each airflow estimate, the min and max values are given. The last column of Table 4 indicates whether or not the synthetic airflow from CONTAM fell within the range of the estimated airflows. For most of the

Table 3: Results of parameter estimation using perfect sensor measurements.

	Synthetic airflow from CONTAM, m^3/h (cfm)	**Airflow from parameter estimation, m^3/h (cfm)**	**Percentage difference (Synthetic – Estimate)/Synthetic × 100**
Q_{0A}	0	0	0%
Q_{A0}	2.25 (79)	2.25 (79)	0.11%
Q_{0B}	0	0	0%
Q_{B0}	2.15 (75)	3.88 (137)	80.93%
Q_{0C}	0	0	0%
Q_{C0}	1.73 (61)	0	100%
Q_{AB}	1.62 (57)	1.63 (57)	0.15%
Q_{BA}	0	0	0%
Q_{AC}	0	0	0%
Q_{CA}	3.88 (136)	3.88 (136)	0%
Q_{BC}	0	0	0%
Q_{CB}	0	0	0%
Q_{RB}	3.63 (128)	1.89 (66)	47.89%
Q_{RC}	14.01 (493)	15.74 (554)	12.38%
ΣQ_{jA}	3.88 (136)	3.88 (136)	0%
ΣQ_{Aj}	3.88 (136)	3.88 (136)	0%
ΣQ_{jB}	5.77 (203)	5.77 (203)	0%
ΣQ_{Bj}	5.77 (203)	5.77 (203)	0%
ΣQ_{jC}	19.62 (690)	19.62 (690)	0%
ΣQ_{Cj}	19.62 (690)	19.62 (690)	0%

Table 4: Results of parameter estimation using sensor measurements with uncertainty.

	Synthetic airflow from CONTAM, m^3/h (cfm)	**Range of airflow from parameter estimation, m^3/h (cfm)**		**Does synthetic value fall within estimated range? (If N, percentage difference)**
		Min	**Max**	
Q_{0A}	0	0	0.04 (1)	Y
Q_{A0}	2.25 (79)	1.97 (69)	2.41 (85)	Y
Q_{0B}	0	0	0.03 (1)	Y
Q_{B0}	2.15 (75)	2.99 (105)	4.73 (166)	N (39-120%)
Q_{0C}	0	0	0.50 (18)	Y
Q_{C0}	1.73 (61)	0	1.21 (42)	N (30-100%)
Q_{AB}	1.62 (57)	0.98 (35)	2.18 (77)	Y
Q_{BA}	0	0	0	Y
Q_{AC}	0	0	0.27 (9)	Y
Q_{CA}	3.88 (136)	3.29 (116)	4.49 (158)	Y
Q_{BC}	0	0	0.81 (28)	Y
Q_{CB}	0	0	1.09 (38)	Y
Q_{RB}	3.63 (128)	0.68 (24)	3.14 (111)	N (13-81%)
Q_{RC}	14.01 (493)	14.5 (509)	17.0 (596)	N (3-21%)
ΣQ_{jA}	3.88 (136)	3.29 (116)	4.53 (159)	Y
ΣQ_{Aj}	3.88 (136)	2.95 (104)	4.87 (171)	Y
ΣQ_{jB}	5.77 (203)	5.13 (180)	7.45 (262)	Y
ΣQ_{Bj}	5.77 (203)	3.67 (129)	8.68 (305)	Y
ΣQ_{jC}	19.62 (690)	19.62 (690)	21.20 (745)	Y
ΣQ_{Cj}	19.62 (690)	17.78 (625)	23.74 (835)	Y

flows, the synthetic airflow from CONTAM does fell within the range of the estimated airflows. Similar to the airflow estimation results with perfect sensor measurements, the estimated range of airflows for Q_{C0}, Q_{B0}, and Q_{RB} did not cover the synthetic values from CONTAM. Neither was it covered for Q_{RC}, though the difference was smaller than for the other three inconsistent airflows. Overall, the magnitude of percentage difference between the synthetic and estimated airflows using sensor measurements with uncertainty was similar to the differences found when using perfect sensor measurements. Therefore, it could be concluded that sensor error did not greatly affect the accuracy of the building airflow network estimate.

The mean absolute difference in estimated airflows was between 0.54 and 0.76 m^3/h (19-21 cfm), which is still < 1 ACH difference in any zone. The largest difference between the steady-state CO_2 concentrations calculated using the estimated airflows and those calculated by the CONTAM model was between 0.4 and 1.1%. This range of error, as a result of using sensor measurements with uncertainty, was very similar to the error as a result of using perfect sensor measurements. Therefore, it could be concluded that sensor error also did not greatly affect the accuracy of the prediction of contaminant concentration.

4. DISCUSSION

Sec. 1.2 indicated four applications for the airflow estimation method presented in this study. First, this study was able to determine the airtightness of each zone, which was nearly identical to the synthetic result calculated by the CONTAM model. Using the estimated airflows, an exfiltration rate of 0.10 ACH existed in Zone B, 0.01 ACH exfiltration in Zone A, and 0 ACH exfiltration in Zone C. The CONTAM model calculated 0.06 ACH exfiltration in Zone B, and 0.01 ACH exfiltration in both Zones A and C. Given that the ventilation supplied 7 ACH to Zones B and C, the differences between the estimated and synthetic exfiltration rates were very small. Therefore, one could reasonably use the results of the estimation method presented in this study to improve the airtightness at specific locations in a building to reduce the amount of energy wasted through infiltration or exfiltration.

Second, this study was able to predict the steady-state CO_2 concentrations within 5% of the synthetic values from CONTAM. Therefore, it could also be reasonably used to predict the transport of other gaseous contaminants. Third, this study was able to determine the pressure distribution inside the synthetic building, which was nearly identical to the synthetic result calculated by the CONTAM model. Using the estimated airflows, it could be concluded that the pressure in Zone C was greater than in Zone A, and the pressure in Zone A was greater than in Zone B. Since it was estimated that there was little to no flow between Zones B and C, one might conclude that the pressures in Zones B and C were equal. However, if that were the case, then the estimate would have shown air from Zone B to Zone A when the opposite was estimated. Therefore, the pressure in Zone B must be the lowest of the three zones and some flow would exist from Zone C to Zone B. Thus, one could reasonably use the results of the estimation method presented in this study to redistribute pressure or select locations for specialized, pressure-sensitive spaces (like in laboratories and hospitals) during a building renovation.

Lastly, the airflow estimation method presented in this study could be used for building commissioning. The airtightness information can be used to help reduce energy waste, the prediction of contaminant dispersion can be used to improve indoor air quality, and the pressure distribution information can be used to verify ventilation performance.

5. CONCLUSIONS

The building airflow network of a synthetic three zone commercial building was estimated using linear least squares with constraints. Steady-state CO_2 measurements were obtained from CONTAM simulations under different occupancy schedules. In Part I of this study, "perfect" steady-state CO_2 measurements were used to estimate the building airflow network. In Part II of this study, the effect of CO_2 sensor uncertainty on the airflow estimate was evaluated. It was found that, no matter without or with sensor uncertainty, steady-state CO_2 measurements were able to be used to obtain a reasonable estimate of the building airflow network compared to the synthetic values from CONTAM. Furthermore, for both parts of this study, even large differences between the synthetic and estimated airflow rates resulted in good prediction of CO_2 concentrations.

6. FUTURE WORK

One area for future work includes utilizing transient CO_2 concentrations to estimate a building airflow network. Recursive least squares (RLS) can be used to estimate airflow based on incoming contaminant data from each zone. RLS offers several advantages over the linear least squares method used in this study. Namely, there is no need for matrix inversion, which is more computationally efficient. To study the effect of sensor uncertainty when utilizing transient CO_2 concentrations, Equation (1) can be rewritten as a stochastic differential equation and then RLS used. Another area for future work includes studying the limitations of the estimation method presented in this study by increasing the number of zones or ACH of the zones. The airflow estimation method presented in this study would also require validation.

REFERENCES

Afonso, C. F. A., Maldonado, E. A. B. and Skåret, E., 1986, A single tracer-gas method to characterize multi-room air exchanges, *Energy and Buildings*, vol. 9, no. 4: p. 273-280.

Aglan, H. A., 2003, Predictive model for CO2 generation and decay in building envelopes, *J.App. Phys.*, vol. 93, no. 2: p. 1287-90.

ASHRAE, 1990, *ANSI/ASHRAE Standard 62-1989: Ventilation for acceptable indoor air quality*, American Society of Heating, Refrigerating and Air-Conditioning Engineers.

ASTM, 2000, *ASTM E741 - 00 Standard Test Method for Determining Air Change in a Single Zone by Means of a Tracer Gas Dilution*, American Society for Testing and Materials.

ASTM, 2003, *ASTM E779 - 03 Standard Test Method for Determining Air Leakage Rate by Fan Pressurization*, American Society of Testing and Materials.

Bahnfleth, W. P., Yuill, G. K. and Lee, B. W., 1999, Protocol for field testing of tall buildings to determine envelope air leakage rate, *ASHRAE Transactions*, vol. 105, no. 2: p. 27-38.

CGSB, 1999, *Determination of the Overall Envelope Airtightness of Buildings by the Fan Pressurization Method Using the Building's Air Handling Systems*, Canadian General Standards Board.

DOC, 2010, Trends in Atmospheric Carbon Dioxide, U. S. Department of Commerce, from http://www.esrl.noaa.gov/gmd/ccgg/trends/.

Jeong, J., Firrantello, J., Bahnfleth, W., Freihaut, J. and Musser, A., 2008, Case studies of building envelope leakage measurement using an air-handler fan pressurisation approach, *Build. Serv. Eng.*, vol. 29, no. 2: p. 137-155.

Lu, T., Knuutila, A., Viljanen, M. and Lu, X., 2010, A novel methodology for estimating space air change rates and occupant CO2 generation rates from measurements in mechanically-ventilated buildings, *Build. Environ.*, vol. 45, no. 5: p. 1161-1172.

Miller, S. L., Leiserson, K. and Nazaroff, W. W., 1997, Nonlinear Least-Squares Minimization Applied to Tracer Gas Decay for Determining Airflow Rates in a Two-Zone Building, *Indoor Air*, vol. 7, no. 1: p. 64-75.

Penman, J. M., 1980, An experimental determination of ventilation rate in occupied rooms using atmospheric carbon dioxide concentration, *Build. Environ.*, vol. 15, no. 1: p. 45-47.

Penman, J. M. and Rashid, A. A. M., 1982, Experimental determination of air-flow in a naturally ventilated room using metabolic carbon dioxide, *Build. Environ.*, vol. 17, no. 4: p. 253-256.

Roulet, C. A. and Foradini, F., 2002, Simple and Cheap Air Change Rate Measurement Using CO2 Concentration Decays, *Int. J. Vent.*, vol. 1, no. 1: p. 39-44.

Smith, P. N., 1988, Determination of ventilation rates in occupied buildings from metabolic CO2 concentrations and production rates, *Build. Environ.*, vol. 23, no. 2: p. 95-102.

Walton, G. N. and Dols, W. S., 2005, *CONTAM 2.4 User Guide and Program Documentation*, National Institute of Standards and Technology.

Yan, Y., Zhipeng, B., Chunrong, J., Zhaofeng, W., Wenting, R. and Jingjing, Z., 2007, Measuring air exchanges rates using continuous CO2 sensors, *Symposium on Air Quality Measurement Methods and Technology 2007, April 30, 2007 - May 3, 2007*, Air and Waste Management Association:p. 101-108.

ACKNOWLEDGEMENT

The authors would like to thank the Koerner Family Foundation for support of this work. Partial support was also provided by the National Science Foundation Graduate Research Fellowship.